Science Advances
AAAS

advances.sciencemag.org/cgi/content/full/6/21/eaba5996/DC1

Supplementary Materials for

Engineered algae: A novel oxygen-generating system for effective treatment of hypoxic cancer

Yue Qiao, Fei Yang, Tingting Xie, Zhen Du, Danni Zhong, Yuchen Qi, Yangyang Li, Wanlin Li, Zhimin Lu, Jianghong Rao, Yi Sun*, Min Zhou*

*Corresponding author. Email: zhoum@zju.edu.cn (M.Z.); yisun@zju.edu.cn (Y.S.)

Published 20 May 2020, *Sci. Adv.* **6**, eaba5996 (2020)
DOI: 10.1126/sciadv.aba5996

This PDF file includes:

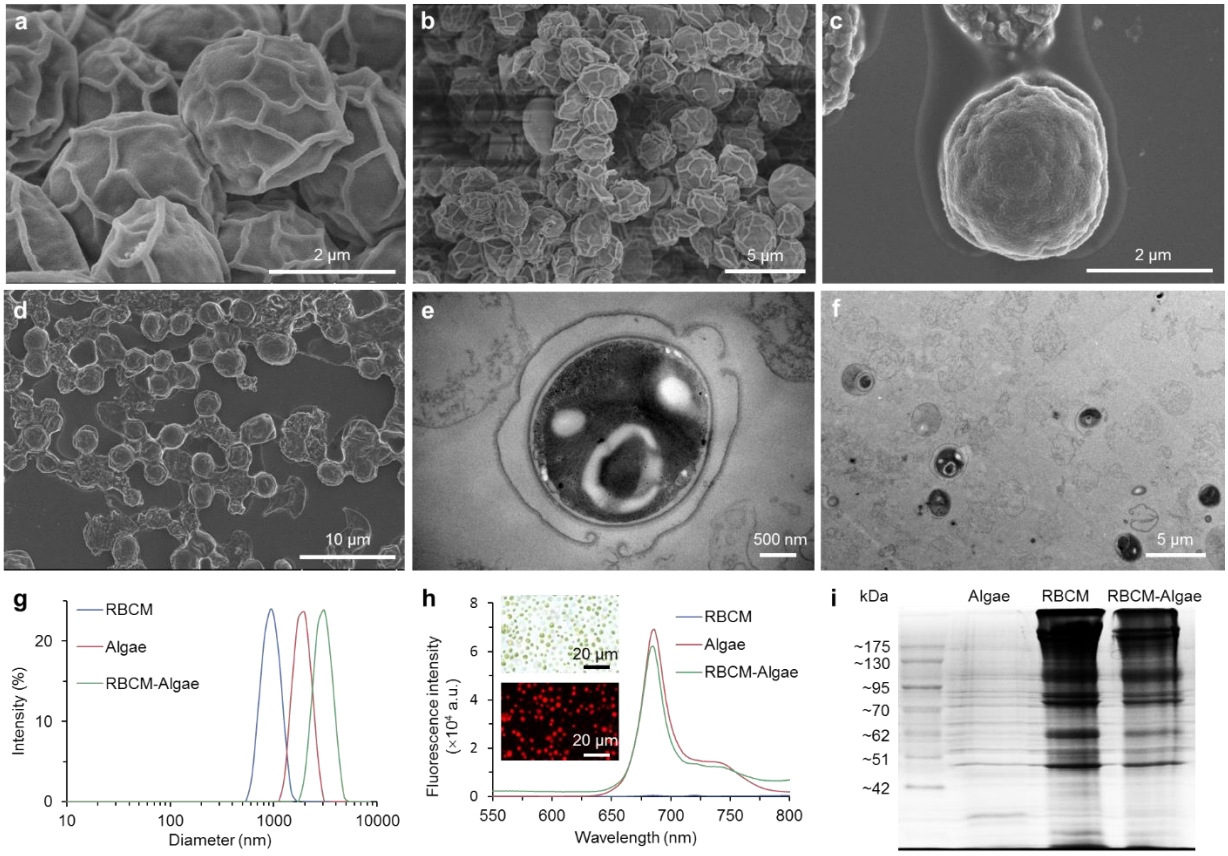

Fig. S1. RBCM could be cloaked on the surface of the algae, which identified in TEM, SEM images, DLS, fluorescence spectra, and SDS-PAGE analysis. (**a,b**) high and low-resolution SEM images of Algae. (**c,d**) high and low-resolution SEM images of RBCM-Algae. (**e,f**) high- and low-resolution TEM images of RBCM-Algae. (**g**) Hydrodynamic diameter distribution of RBCM, Algae, and RBCM-Algae. (**h**) Fluorescence emission spectra of RBCM, Algae, and RBCM-Algae. Bright-field and fluorescence micrograph of RBCM-Algae (inset). (**i**) Images of SDS-PAGE gels showing protein contents in RBCM, Algae, and RBCM-Algae.

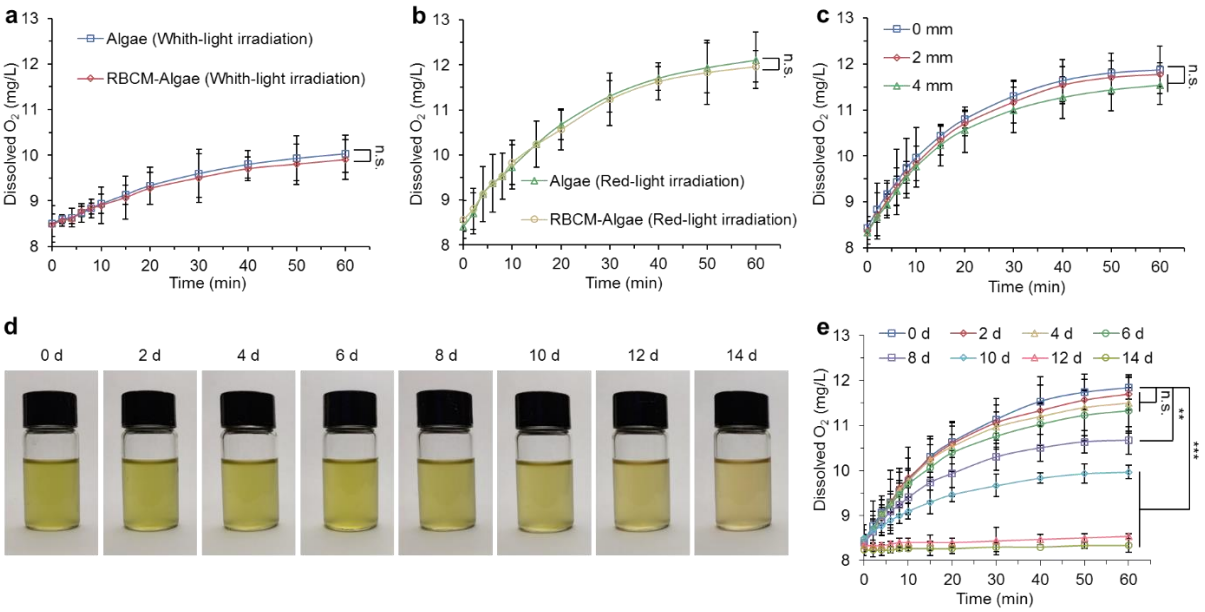

Fig. S2. RBCM-Algae have similar oxygenation characteristics to normal algae, penetration depth assay of red light and stability analysis. More O_2 could be generated by RBCM-Algae under red-light irradiation. There are no significant differences in the O_2 generation capacity of Algae and RBCM-Algae under (**a**) white light (6000 Lux) and (**b**) red light (6000 Lux) illumination. (**c**) The oxygenation of RBCM-Algae (5×10^7/mL) under red light irradiation with block of different thicknesses (2 and 4 mm) of chicken breast. RBCM-Algae (5×10^7/mL) were stored at 4 °C for 2 weeks after preparation. (**d**) Photographs of RBCM-Algae during 2 weeks. (**e**) Storage time-dependent oxygenation of the RBCM-Algae under red light. Data are means ± SD, n = 3, t-Student two tail test, n.s. $p \geq 0.05$, *$p < 0.05$, **$p < 0.01$, ***$p < 0.001$. Figure S2D ("Photo Credit: Min Zhou, Zhejiang University").

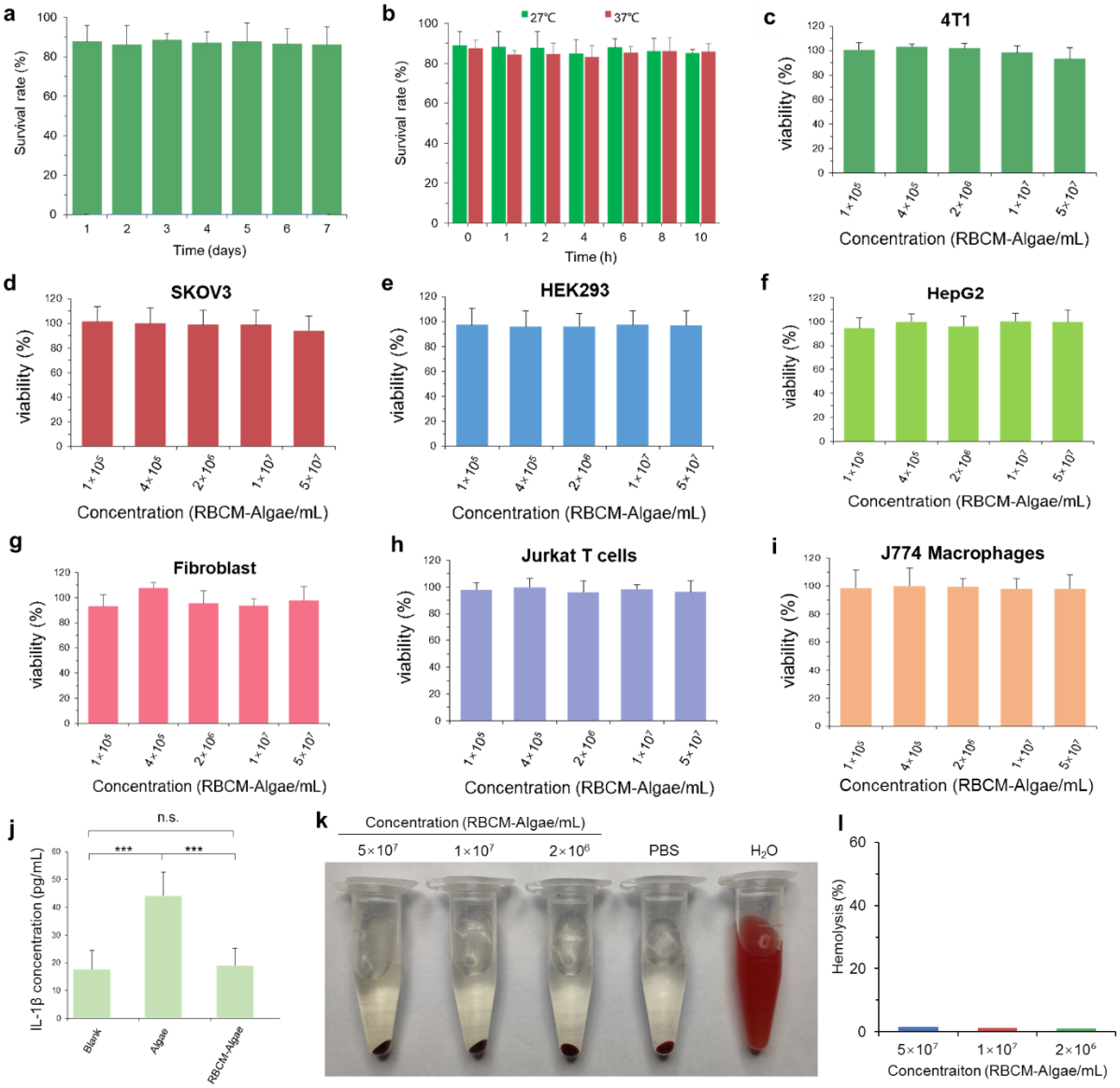

Fig. S3. RBCM-Algae possesses high survival rates in physiological environments, showing no obvious cytotoxicity to various cells, no immunological effects on macrophages and hemolytic biocompatibility. (**a**) Survival rate of RBCM-Algae with time variation in a long-term period. (**b**) Survival rate of RBCM-Algae at 27 °C and 37 °C with time variation in a short-term experiment. (**c-i**) Viability of various cells (4T1, SKOV3, HEK293, HepG2, Fibroblast, Jurkat T and J774 cells) treated with RBCM-Algae at different concentrations. (**j**) Cytokine level produced by J774 macrophages after incubation with RBCM-Algae for 24 hrs. (**k**) Images of blood of mice incubated with a series of concentration of RBCM-Algae. PBS and diH_2O as the positive and negative controls, respectively. (**l**) Corresponding quantification of hemolysis percent. Data are means ± SD, n = 3, t-Student two tail test, n.s. $p \geq 0.05$, *$p < 0.05$, **$p < 0.01$, ***$p < 0.001$. Figure S3K ("Photo Credit: Min Zhou, Zhejiang University").

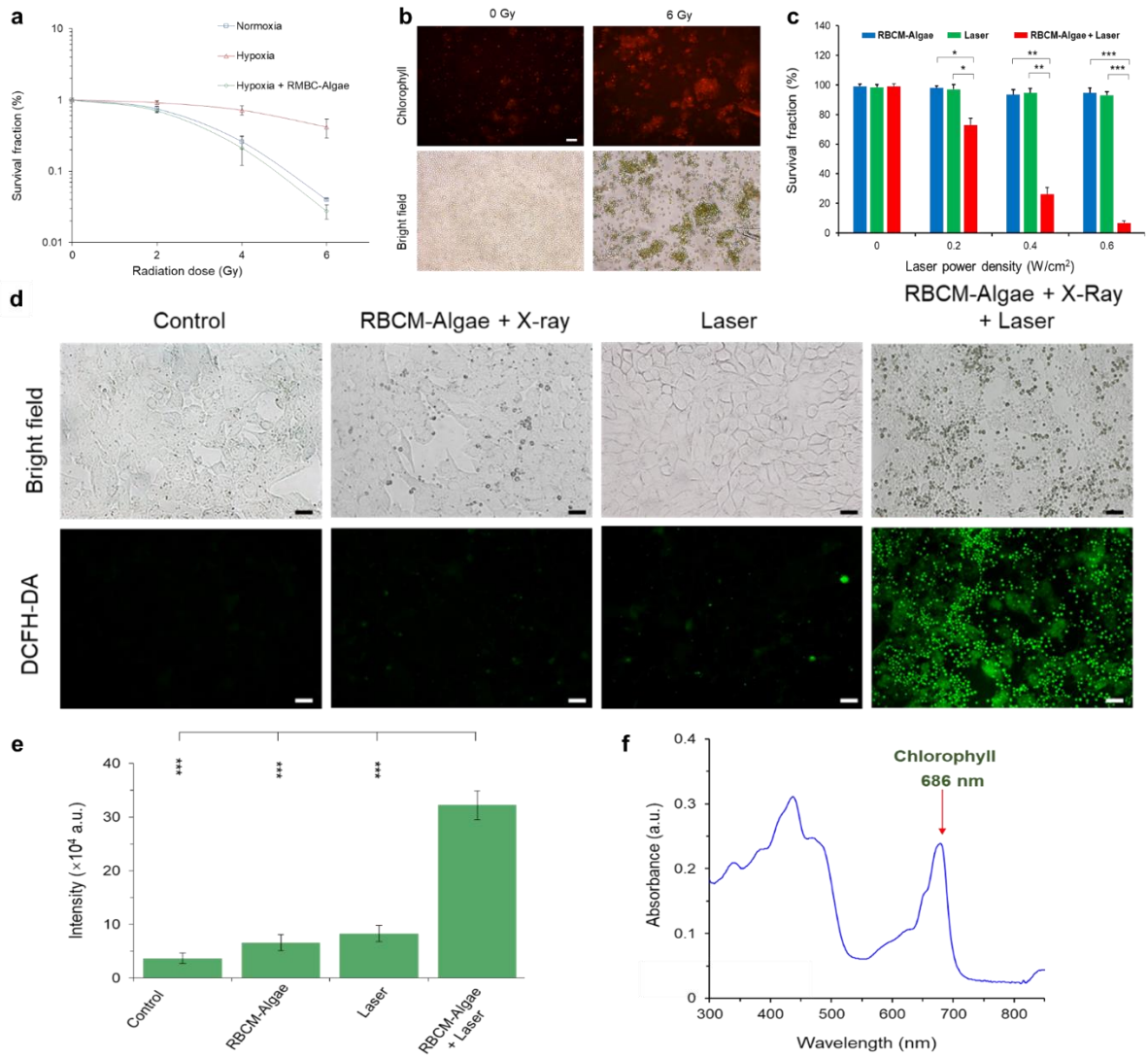

Fig. S4. Chlorophyll was release after the X-ray treatment, more cancer cells were killed caused RBCM-Algae could produce ROS effects under the 650-nm laser irradiation. (**a**) Quantification of the corresponding survival fractions of Fig. 2b. (**b**) Compare to no treatment, much more strong chlorophyll was found after X-ray treatment (6 Gy). (**c**) The corresponding quantitative analysis of the survival fraction of Fig. 2h. (**d**) ROS assay in vitro with different treatments on 4T1. Fluorescent via DCFH-DA stained (green, generated ROS) and bright-field micrographs. (**e**) The corresponding quantitative analysis of the fluorescence intensity. (**f**) the optical absorbance of RBCM-Algae. Data are means ± SD, n = 3, t-Student two tail test, n.s. $p \geq 0.05$, *$p < 0.05$, **$p < 0.01$, ***$p < 0.001$.

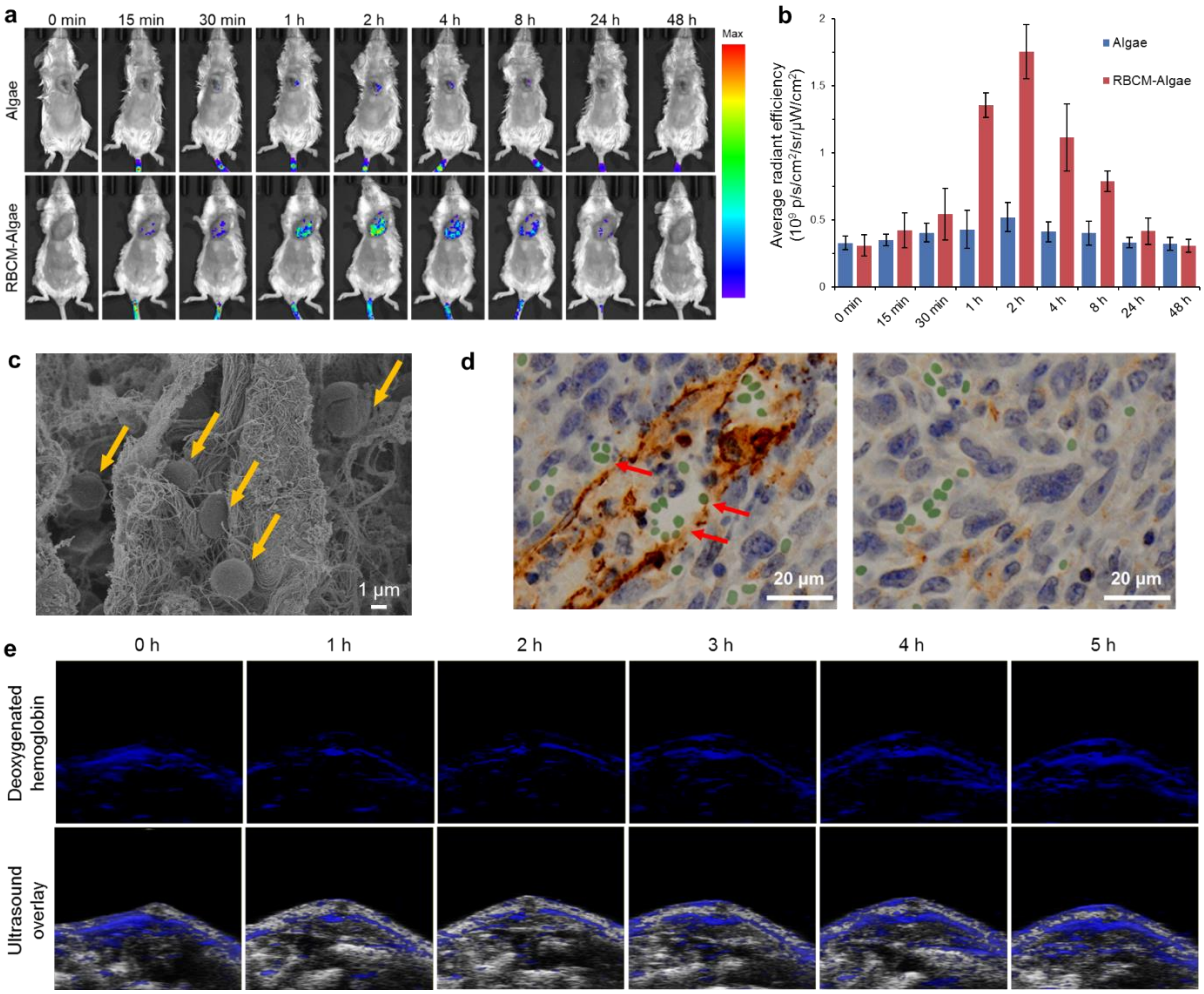

Fig. S5. More RBCM-Algae could accumulate in the tumor, were clearly found in the tumor tissue and reduced hypoxia *in vivo* after i.v. injection. (**a**) *In vivo* fluorescence images at different time points after i.v. administration of Algae and RBCM-Algae, respectively in 4T1 tumor-bearing mice and (**b**) the corresponding quantitative analysis. (**c**) High-resolution grayscale SEM micrograph before false coloring of RBCM-Algae locating in 4T1 tumor after in vivo tumor targeting through i.v. administration, red arrow: algae. (**d**) CD31 staining of lung tissue sections. Tumor vasculature was stained in brown, and red arrows point to RBCM-Algae. (**e**) Photoacoustic images of deoxygenated hemoglobin in 4T1 tumor at different time points after i.v. administration of RBCM-Algae. Data are means ± SD, n = 3.

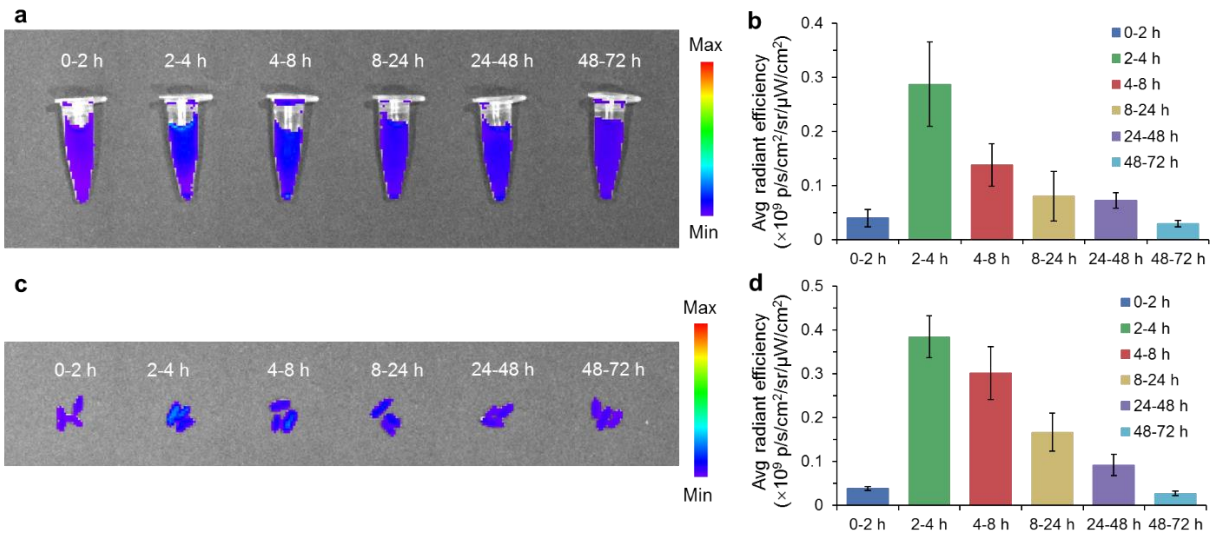

Fig. S6. Excretion analysis after i.v. injection. (a) *Ex vivo* imaging of urine for renal clearance (b) and the quantitative analysis. (c) *Ex vivo* imaging of feces for hepatic metabolism (d) and the quantitative analysis. Data are means ± SD, n = 3.

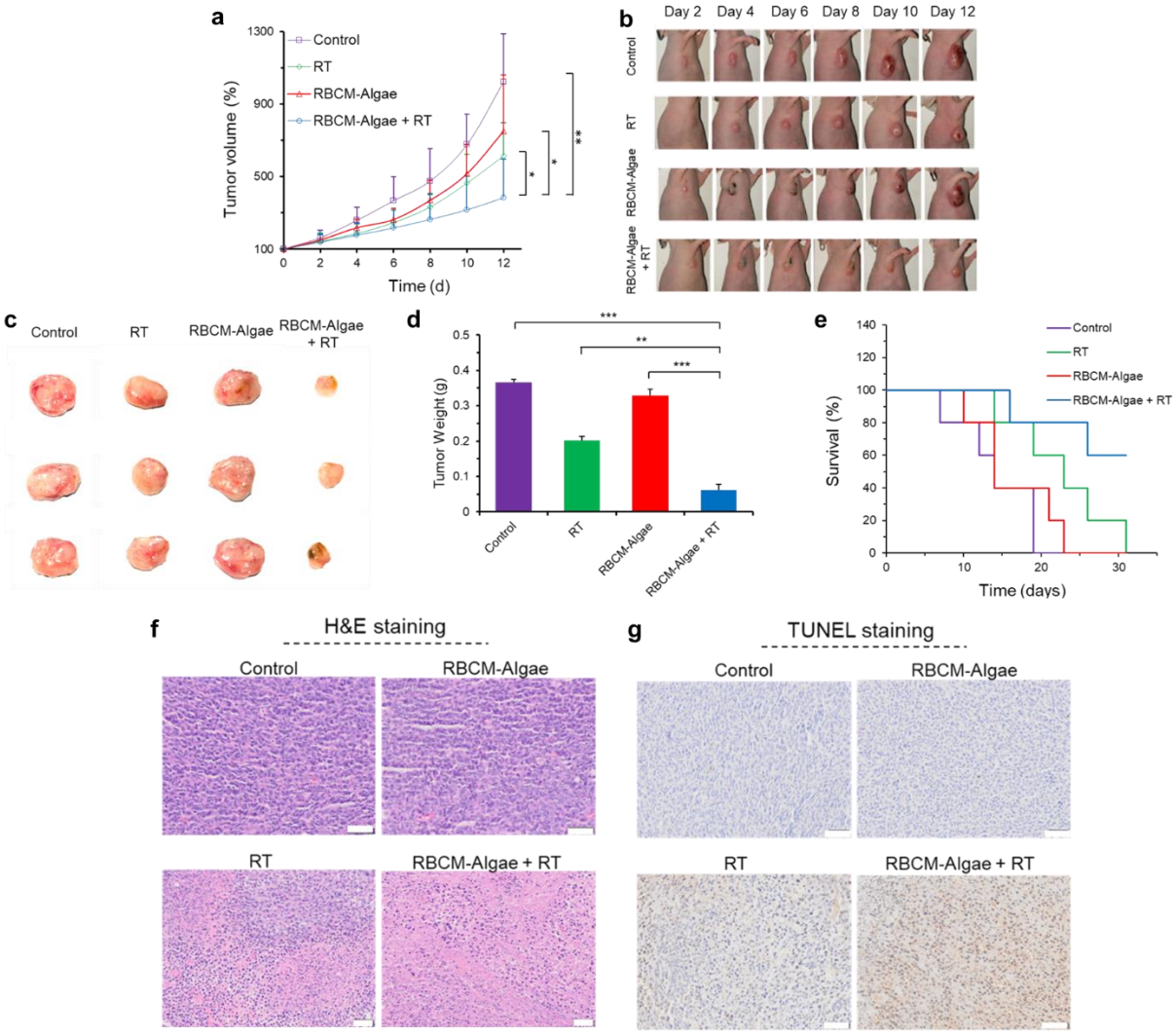

Fig. S7. RBCM-Algae could enhance the radiotherapeutic effects in 4T1 breast tumor model and more necrosis and apoptosis in the tumor treated by RBCM-Algae mediated radiotherapy. (**a**) tumor growth curves, (**b**) photographs of animals, (**c**) photograph of tumor tissues, (**d**) tumor weights, (**e**) animal survival curves. The volumes and weights of tumors in the mice receiving RBCM-Algae+RT treatment are significantly smaller than that of the mice in all the other three groups. The mice in the RBCM-Algae+RT group also demonstrated a longer survival span than the other groups. No significant body weight changes among all the mice in various treatments were found. (**f**) H&E staining, (**g**) TUNEL staining. Both H&E and TUNEL staining demonstrated severe tumor tissues damages in the RBCM-Algae+RT group. Bar: 50 μm. Data are means ± SD, n = 3, t-Student two tail test, n.s. $p \geq 0.05$, *$p < 0.05$, **$p < 0.01$, ***$p < 0.001$. Figure S7B and S7C ("Photo Credit: Min Zhou, Zhejiang University").

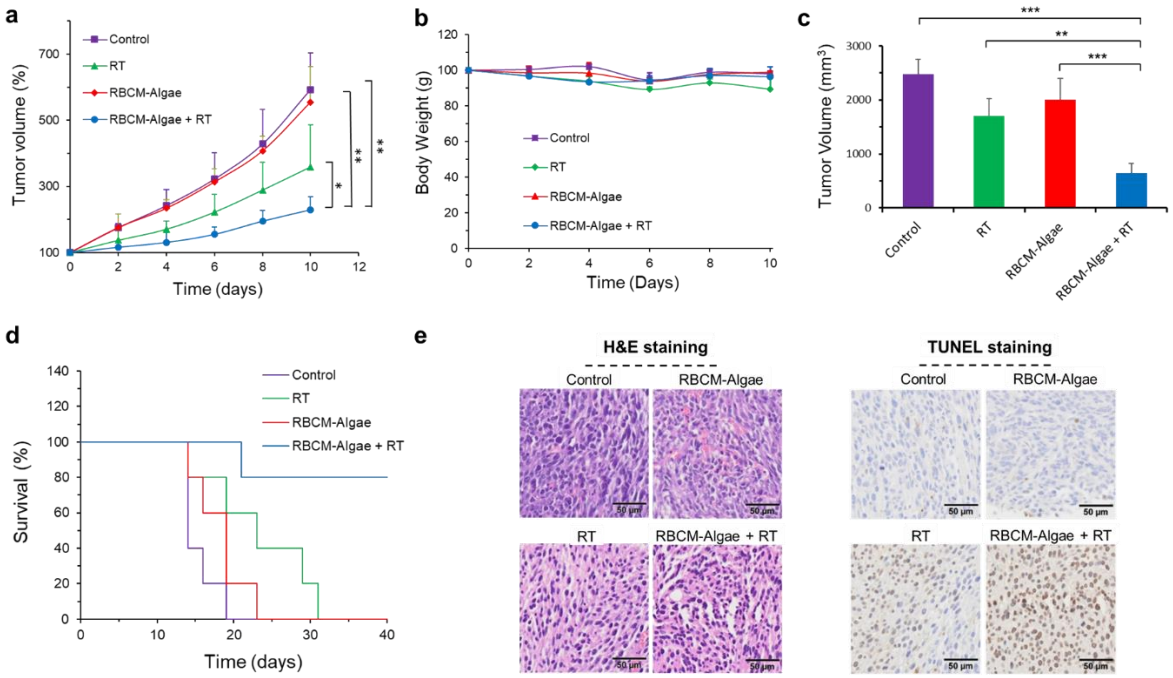

Fig. S8. RBCM-Algae could enhance the radiotherapeutic effects in SKOV3 ovarian tumor model and histological analysis of tumor tissues. (**a**) Tumor growth curves, (**b**) body weights, (**c**) tumor volumes, and (**d**) animal survival curves. In the SKOV3 ovarian tumor model, the tumor growth curves of the mice demonstrated the best therapeutic effects of RBCM-Algae+RT treatment group. The tumor volumes were significantly smaller than the volumes of the mice in all the other three groups, the survival of the mice in this group also demonstrated longer survival span than the other groups, indicating the best therapeutic effect by RBCM-Algae+RT treatment. Also, no significant body weight changes of all the mice in various treatments were found. (**e**) Representative H&E staining of tumor sections in different treatment groups (day 10) and corresponding quantitative analysis. Data are means ± SD, n = 3, t-Student two tail test, n.s. $p \geq 0.05$, *$p < 0.05$, **$p < 0.01$, ***$p < 0.001$.

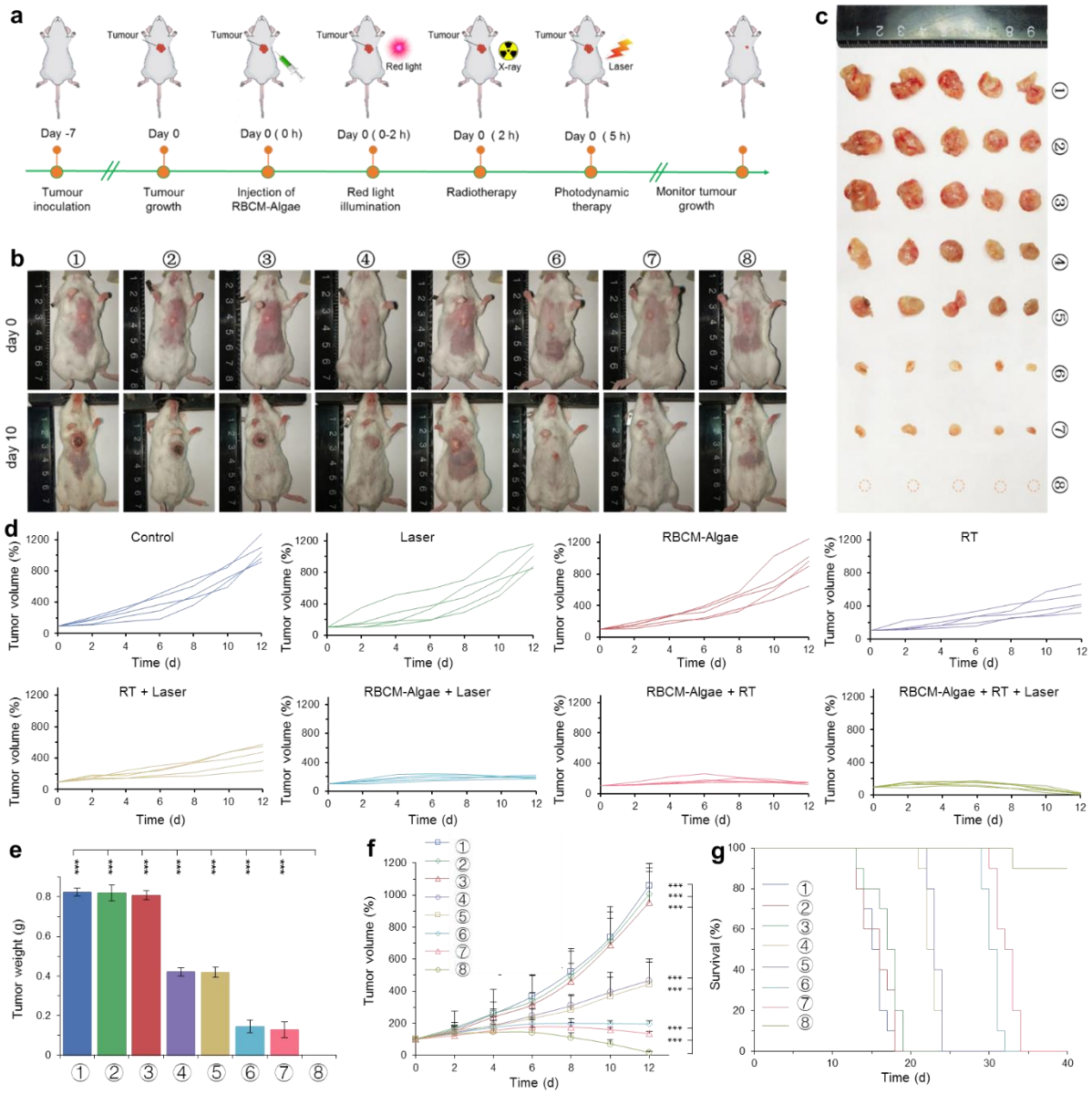

Fig. S9. Engineered algae mediated radiotherapy and photodynamic therapy can inhibit efficiently the tumor growth (4T1 breast cancer model) after i.t. injection. (**a**) Scheme illustrating treatments. (**b**) photograph of the treated mice, (**c**) photograph of tumors, and (**e**) tumor weights. For the i.t. injection experiment, the tumor weights of the mice in the RBCM-Algae+RT+Laser treatment group were significantly smaller than the volumes of the mice in all the other three groups, indicating the best therapeutic effect by RBCM-Algae+RT treatment. (**d**) tumor growth curves of each group, (**f**) tumor growth of all groups, (**g**) animal survival curves. For the i.t. injection experiment, the tumor growth curves and survival of the mice in the RBCM-Algae+RT+Laser treatment group demonstrated the best therapeutic effect in all the other groups. Data are means ± SD, n = 3, t-Student two tail test, n.s. $p \geq 0.05$, *$p < 0.05$, **$p < 0.01$, ***$p < 0.001$. Figure S9B and S9C ("Photo Credit: Min Zhou, Zhejiang University").

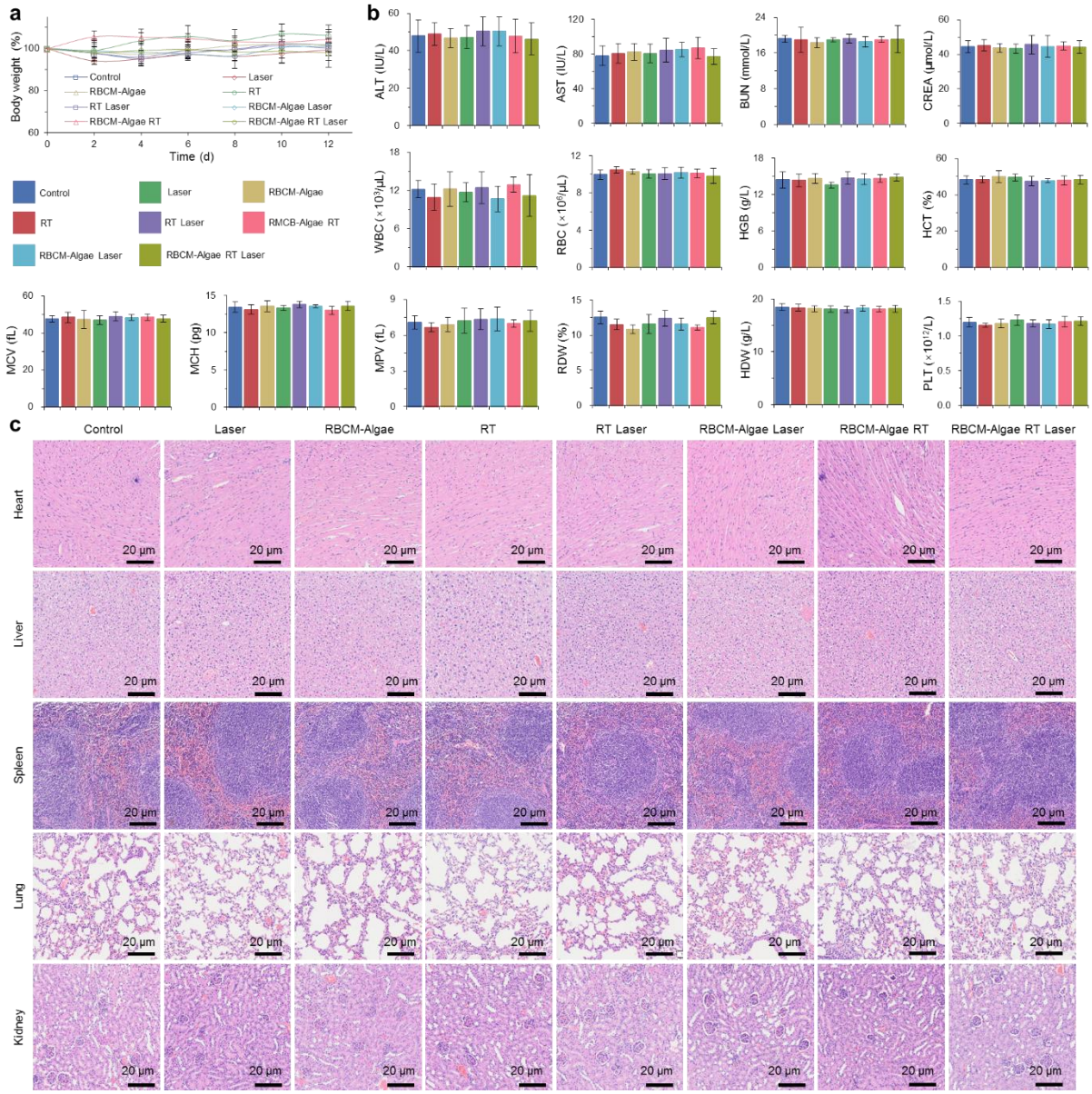

Fig. S10. Preliminary toxicity analysis: Body weights, blood chemistry analysis and histological analysis of major organs. RBCM-Algae (5 x 10^7) were i.v. injected into the Balb/c mouse. (**a**) body weights of the mice were recorded. (**b**) The blood samples were collected after 12 days for the further analysis. Red blood cells (RBC), hemoglobin (HGB), white blood cells (WBC), red cell distribution width (RWD), hematocrit (HCT), mean platelet volume (MPV), mean corpuscular hemoglobin (MCH), and mean corpuscular hemoglobin concentration (MCHC) were analyzed. Liver function was evaluated by determining the serum levels of alanine aminotransferase (ALT), and aspartate aminotransferase (AST). Kidney function was determined by measuring the serum blood urea nitrogen (BUN) and creatinine (CREA) levels. Compared to mice with various treatments, no statistical difference was observed in any of the parameters, including blood chemistry and major blood cell populations) that were studied. (**c**) H&E staining of major organs, including heart, liver, spleen, lung, and kidney. Analysis after H&E staining revealed normal appearance in all the organs studied, including the liver, spleen, heart, lungs, and kidneys. Data are means ± SD, n = 5.